Normal Force Exerted on Vascular Endothelial Cells

Yechun Wang and P. Dimitrakopoulos*

Department of Chemical and Biomolecular Engineering, University of Maryland, College Park, Maryland 20742, USA

(Received 19 April 2005; published 18 January 2006)

Hemodynamic forces play an important role in the normal and pathological behavior of vascular endothelial cells as recent studies on the shear stress over the endothelium have shown. Based on computational investigation and scaling analysis, our study shows that the normal force contributes significantly to the total force on the endothelial cells even in large vessels. Therefore, our study suggests that the functions of endothelial cells are also affected by the normal forces exerted on them. The effects of the normal force are more pronounced for smaller vessels and/or less spread cells.

DOI: 10.1103/PhysRevLett.96.028106 PACS numbers: 87.10.+e, 87.16.Ac, 87.16.Dg, 87.19.Uv

Hemodynamic forces play a pivotal role in the normal and pathological behavior of vascular endothelial cells. A plethora of studies, mainly in the last two decades, has attributed the behavior, or changes in the behavior, of the endothelium as a result of one of the two components of the hemodynamic force, i.e., as effects of the shear stress. For example, the production of prostacyclin and nitric oxide was found to be affected by the type of shear stress on the endothelium [1,2]. Shear stress was also found to increase the endothelial hydraulic conductivity through signal transduction [3] and to regulate occludin content and phosphorylation [4]. The ability of endothelial cells to induce adhesion and migration of flowing neutrophils was found to be affected by the magnitude of shear stress in the presence of tumor necrosis factor a [5]; this ability was also found to be affected by oscillatory shear stress [6]. The endothelial surface layer (glycocalyx) acts as a mechanotransducer of the fluid shear stress to the actin cortical cytoskeleton of the endothelial cells [7]. The biomechanical forces also affect the endothelial structure and function such as the permeability to macromolecules, lipoprotein accumulation, and the repair near branch points [8]. In addition, shear stress acting at the endothelium surface was found to produce rapid deformation of stable intermediate filament networks [9]. Thus, the influence of the second component of the hydrodynamic force on the endothelium, i.e., the normal force or pressure, has been overlooked. This study shows that the normal force contributes significantly to the total force on the endothelial cells even at large vessels. Therefore, our study suggests that the behavior of endothelial cells in capillaries, arterioles, and venules as well as in arteries and veins is also affected by the normal force exerted on them.

To investigate the shear and normal force over vascular endothelial cells in vessels with diameter comparable or larger to the size of the cell, we consider Stokes flow of a Newtonian fluid around a solid spherical-cap protuberance in a cylindrical vessel of radius R as shown in Fig. 1. We emphasize that since the cell size is a few microns, i.e., O (μm), if we consider flow in capillaries (with a typical diameter of 8 μm) as well as in arterioles and venules (with a typical diameter of 10–140 μm) [10], we have to explicitly consider the curvature of the vessel wall. In addition, due to the small size of the cell and/or the vessel, the assumption of Stokes flow is well justified [10–12]. The assumption of the Newtonian surrounding fluid is rather well justified based on recent results for the similar problem of leukocyte adhesion in cylindrical vessels which showed that the difference in modeling the surrounding fluid as either Newtonian or non-Newtonian is rather small [13]. We emphasize that the intercell influence is weak due to the fast decay of the perturbation force on the cell and the large intercell distance with respect to the cell size [11].

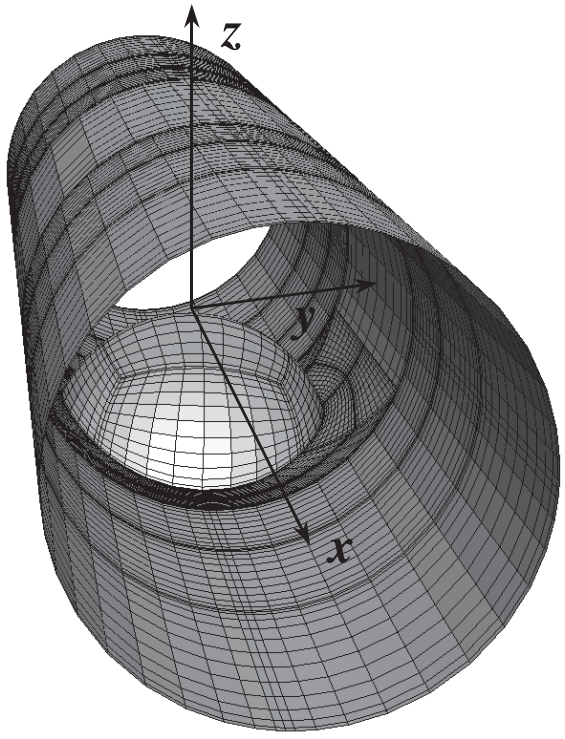

FIG. 1. An endothelial cell on the inner surface of a cylindrical vessel.

Thus, our simplified model is able to capture the important physics of the complicated realistic problem.

The Stokes flow around the cell may be described by the boundary integral equation

$$\boldsymbol{u} = -\frac{1}{4\pi\mu}\int_S [\boldsymbol{S}\cdot\boldsymbol{f} - \mu\boldsymbol{T}\cdot\boldsymbol{u}\cdot\boldsymbol{n}]dS, \qquad (1)$$

where μ is the viscosity of the surrounding fluid (e.g., see [14]). This equation relates the velocity $\boldsymbol{u}$ at each point on the boundary S as a surface integral of the force vector $\boldsymbol{f}$ and the velocity $\boldsymbol{u}$ over all points on the same boundary. (Note that the tensors $\boldsymbol{S}$ and $\boldsymbol{T}$ are known functions of geometry [14], while the unit normal $\boldsymbol{n}$ points into the domain volume surrounded by the boundary S.) For the current problem the surface S consists of the solid surface S_s of the cell and the microvessel wetted by the surrounding fluid as well as the fluid surface S_f of the vessel's inlet and outlet far away from the cell. The relevant boundary conditions are $\boldsymbol{u} = 0$ on the solid boundary S_s, and $\boldsymbol{u} = \boldsymbol{u}^\infty$ or $\boldsymbol{f} = \boldsymbol{f}^\infty$ on the fluid boundary S_f, where $\boldsymbol{f}^\infty$ is the force associated with the undisturbed Poiseuille flow $\boldsymbol{u}^\infty$ far from the cell. The numerical solution of the boundary integral equation (1) is achieved through the spectral boundary element method [15,16].

The cell is modeled as a spherical cap whose size is specified by its volume V or equivalently by the radius $\tilde{a}$ of a spherical volume $V = (4\pi/3)\tilde{a}^3$. Because of the vessel's cylindrical shape, the spreading angle at the intersection of the cell surface with the vessel surface varies with the azimuthal angle. For a given size $\tilde{a}/R$ of a spherical-cap cell, the relationship between the spreading angle θ and the azimuthal angle ϕ may be determined by the spreading angle θ_0 at $\phi = 0°$. (In this study, θ_0 is defined from within the cell; i.e., for a fully spread cell $\theta_0 = 0°$, while a nonspread cell has $\theta_0 = 180°$; the azimuthal angle ϕ is measured with respect to the positive x direction depicted in Fig. 1.) Note that for a given cell volume V, the two dimensionless parameters of the current problem, i.e., $\tilde{a}/R$ and θ_0, are independent.

Figure 2 shows that the total force F_x exerted on the cell along the flow direction increases with the cell size $\tilde{a}/R$ for any spreading angle as well as with the spreading angle θ_0 for moderate and large cell sizes. The increase is much more pronounced at large cell sizes and spreading angles due to the resulting higher blocking to the vessel flow. For small cell sizes, increasing the spreading angle from small values the total force F_x decreases up to $\theta_0 \approx 50°$ as shown in the figure's inset; for higher values of θ_0 the total force increases with the spreading angle.

To investigate further on the nature of the force exerted on the cell, we separated the total force on the cell into its two components, i.e., the shear force F_x^{shear} and the normal force F_x^n. The relative contribution of the two force components to the total force is shown in Fig. 3. For large vessels (i.e., small $\tilde{a}/R$) the shear force F_x^{shear} contributes more to the total force than the normal force F_x^n, but the contribution of the normal force cannot be neglected especially at large spreading angles. (For example, even for $\tilde{a}/R \to 0$ the normal force on the cell is 30% of the shear force for $\theta_0 = 60°$, and close to 56% for $\theta_0 = 120°$.) As the vessel radius decreases (i.e., $\tilde{a}/R$ increases), the relative contribution of the normal force increases and at large cell sizes $\tilde{a}/R$ becomes dominant. The increase of the relative contribution of the normal force with the cell size is much faster for large spreading angles. (For $\theta_0 = 120°$ and $\tilde{a}/R = 0.9$, F_x^n is more than 4 times greater than the shear force.)

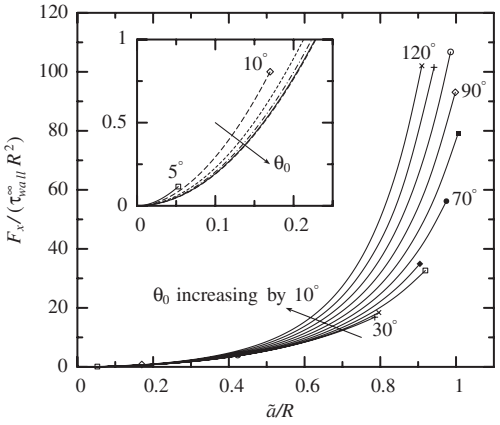

FIG. 2. The total force F_x exerted on the cell as a function of the cell size $\tilde{a}/R$ for spreading angles $\theta_0 = 5°, 10°, 20°, \ldots, 120°$ (increments of 10°). The inset shows the same variation for small and moderate angles $\theta_0 = 5°, 10°, 20°, \ldots, 50°$. (Note that $\tau_{\text{wall}}^{\infty}$ is the undisturbed shear stress on the vessel wall far from the cell.)

To understand further the nature of the shear and normal force on the cell, we provide a scaling analysis for these two forces as functions of the cell size and the spreading angle. Since our interest is to understand the increase of the normal force contribution as the vessel radius decreases

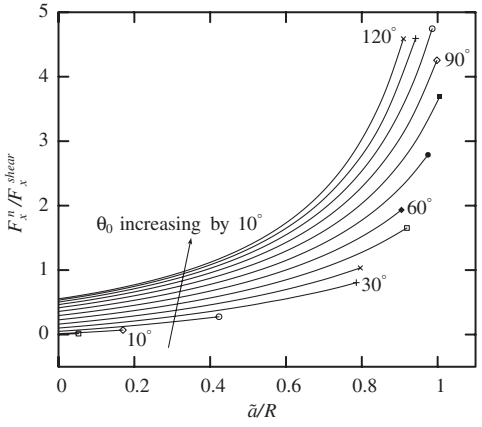

FIG. 3. Relative importance of the normal force F_x^n with respect to the shear force F_x^{shear} exerted on the cell versus the cell size $\tilde{a}/R$ for the same set of parameters as in Fig. 2.

from large values, our scaling analysis is formally valid for small cell sizes $\tilde{a}/R$.

The shear force F_x^{shear} on the cell is proportional to the shear stress on the cell τ_c and the cell's surface area S_c. For small spreading angles θ_0 and small cell sizes $\tilde{a}/R$, the cell's surface area S_c is proportional to the contact region $A_c \sim \ell_x \ell_y$, where ℓ_x and ℓ_y are the length and the width of the cell, respectively, while for our problem $\ell_x \sim \ell_y$. Based on the cell's volume, we have $V \sim \tilde{a}^3 \sim \ell_x \ell_y \ell_z$ where the cell's height $\ell_z \sim \ell_x \tan\theta_0 \sim \ell_x \theta_0$ for small angles; thus $\ell_x \sim \ell_y \sim \tilde{a}\theta_0^{-1/3}$, $\ell_z \sim \tilde{a}\theta_0^{2/3}$, and $S_c \sim \tilde{a}^2\theta_0^{-2/3}$. The shear stress τ_c on the cell is proportional to the undisturbed shear stress on the vessel wall far from the cell $\tau_{\text{wall}}^{\infty}$. Thus for small angles and cell sizes, the shear force on the cell scales as

$$F_x^{\text{shear}} \sim \tau_c S_c \sim \tau_{\text{wall}}^{\infty} \tilde{a}^2 \theta_0^{-2/3}. \tag{2}$$

The scaling analysis predicts that the shear force F_x^{shear} decreases with increasing the spreading angle due to the associated decrease of the cell's surface area S_c. This conclusion is in agreement with our numerical results for angles up to $\theta_0 \approx 70°$ shown in the inset of Fig. 4; for higher θ_0 the shear force shows a monotonic increase with the spreading angle as seen in Fig. 4.

The normal force F_x^n on the cell may be divided into two distinct components. The first term F_x^{n1} arises from the undisturbed pressure gradient acting on the cell. For small spreading angles θ_0 and small cell sizes $\tilde{a}/R$, the pressure gradient in the flow direction scales as $\tau_{\text{wall}}^{\infty}/R$. The corresponding pressure change over the cell scales as $\Delta p^1 \sim \tau_{\text{wall}}^{\infty} \ell_x / R \sim \tau_{\text{wall}}^{\infty} (\tilde{a}/R) \theta_0^{-1/3}$. The force component F_x^{n1} is proportional to Δp^1 and the frontal area of the cell, $A_f \sim \ell_y \ell_z \sim \tilde{a}^2 \theta_0^{1/3}$. Therefore, for small cell sizes and small spreading angles the first normal force component scales as

$$F_x^{n1} \sim \Delta p^1 A_f \sim \tau_{\text{wall}}^{\infty} \frac{\tilde{a}^3}{R}; \tag{3}$$

i.e., it is independent of the spreading angle. The other component of the normal force F_x^{n0} arises from the disturbance of the base flow owing to the presence of the cell. The pressure change Δp^0 for this term scales as $\tau_{\text{wall}}^{\infty}\theta_0$, and thus the associated normal force scales as

$$F_x^{n0} \sim \Delta p^0 A_f \sim \tau_{\text{wall}}^{\infty} \tilde{a}^2 \theta_0^{4/3}. \tag{4}$$

The component of the normal force due to the undisturbed pressure gradient F_x^{n1} is negligible at very small cell sizes due to its $\tilde{a}/R$ dependence but becomes the dominant component as the cell size increases. On the other hand, the base normal force component F_x^{n0} is negligible compared to the dominant pressure gradient component F_x^{n1} at moderate and large cell sizes; only for small cell sizes is F_x^{n0} expected to affect the normal force on the cell. For example, for all angles studied in this Letter, the normal force is proportional to $\tilde{a}^3/R$ for moderate cell sizes due to the pressure gradient component F_x^{n1}; on the other hand, for small $\tilde{a}/R$ our numerical results show that $F_x^n \sim \tilde{a}^2$, in agreement with our aforementioned analysis on the base normal component F_x^{n0}. The influence of the spreading angle θ_0 on the normal force F_x^n is shown in Fig. 5; in contrast to the shear force, F_x^n increases monotonically with both the cell size $\tilde{a}/R$ and the spreading angle θ_0; the increase is much more pronounced at high cell sizes and spreading angles.

Based on our analysis presented above, the explanation for the behavior of the two force components is now straightforward. At small cell sizes, the decrease of the total force F_x on the cell with increasing spreading angle for small and moderate angles θ_0 (shown in the inset of Fig. 2) is caused by the dominant shear component F_x^{shear} and thus by the associated decrease of the cell's surface area. The rapid increase of F_x at large cell sizes and spreading angles shown in Fig. 2 results mainly from the

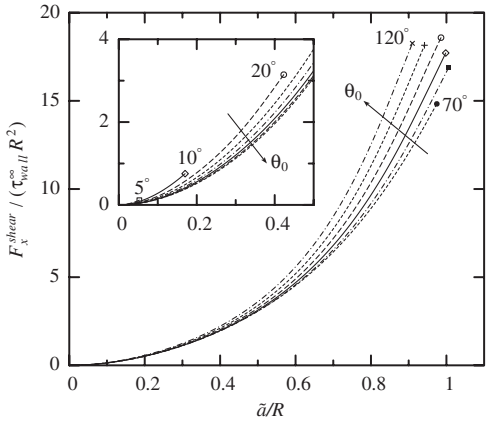

FIG. 4. The shear force F_x^{shear} exerted on the cell as a function of the cell size $\tilde{a}/R$. The spreading angle θ_0 varies from 70° to 120° in increments of 10°. The inset shows the same variation for small and moderate angles 5°, 10°, 20°, ..., 70°.

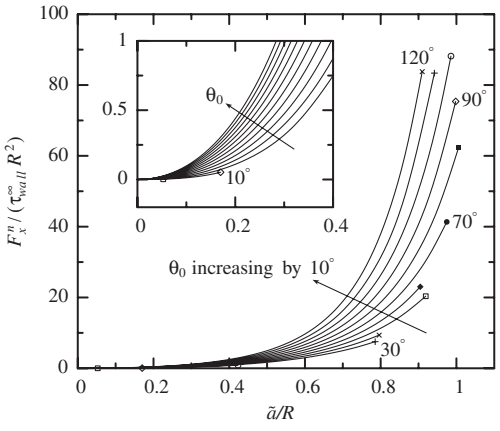

FIG. 5. The normal force F_x^n exerted on the cell as a function of the cell size $\tilde{a}/R$ for the same set of parameters as in Fig. 2. The inset shows the same variation for small cell sizes $\tilde{a}/R$.

normal force F_x^n exerted on the cell. At small cell sizes $\tilde{a}/R \to 0$, the relative importance of the normal force with respect to the shear force exerted on the cell scales as $F_x^n/F_x^{\text{shear}} \sim \theta_0^2$ based on Eqs. (2) and (4); i.e., it increases with the spreading angle as shown in Fig. 3. At larger cell sizes, the rapid increase of the ratio F_x^n/F_x^{shear} results from the contribution of the pressure gradient normal force F_x^{n1}.

For all cell sizes $\tilde{a}/R$, the contribution of the normal force on the cell cannot be neglected, especially for less spread cells as shown clearly in Fig. 3 even though the normal force may change nature as the cell size varies. At moderate and large cell sizes, the pressure gradient normal force F_x^{n1} contributes significantly to the total force on the cell and even becomes the dominant component at small vessels (see Fig. 3). At very small cell sizes $\tilde{a}/R$ (or at large vessel radius for a given cell), Eq. (2) shows that the shear force F_x^{shear} is independent of the vessel radius R; the same is true for the normal force since in this case the pressure gradient normal force F_x^{n1} is negligible and thus F_x^n is dictated by its base pressure component F_x^{n0} which is independent of the vessel radius as Eq. (4) reveals. Thus, for large vessels the curvature of the vessel's wall can be neglected (i.e., one may model the vessel as a plane). However, even in this case, the contribution of the normal force F_x^{n0} should be taken into account in the determination of the total force on the cell as Fig. 3 shows for $\tilde{a}/R \to 0$. We emphasize that the base pressure component F_x^{n0} results from the anomaly of the vessel surface due to the presence of the endothelial cell and thus exists for any vessel (see our scaling analysis above).

The conclusions above are in direct contrast to the common practice of previous studies which attribute the operation of endothelial cells to the shear stress exerted on them, and thus neglect the normal force contribution. (For example, see Refs. [1–9] while additional references may be found in these publications.) Since both normal and shear forces can affect the stretching and bending of the cell membrane (see references on cell membranes, e.g., [17]), our study suggests that both the normal and the pathological behavior of endothelial cells are affected by the normal force exerted on them. We hope that our study motivates experiments, both *in vitro* and *in vivo*, to identify the effects of the normal force on the functions of the endothelial cells in blood vessels, especially from small arteries and veins down to capillaries where the contribution of the normal force is expected to be significant and/or dominant due to its pressure gradient component. For moderate and small size vessels, it would be better for *in vitro* experiments to approximate the vessel as a tube rather than as a parallel plate device, since the latter device underestimates the true normal force on the cells by providing flow blocking along only one direction, i.e., the distance of the plates.

This work was supported in part by the National Science Foundation. Acknowledgment is made to the Donors of the American Chemical Society Petroleum Research Fund for partial support of this research. Some computations were performed on the multiprocessor computers IBM pSeries 690 and Xeon Linux Supercluster provided by the National Center for Supercomputing Applications (NCSA) in Illinois.

*Electronic address: dimitrak@eng.umd.edu

[1] J. A. Frangos, S. G. Eskin, L. V. McIntire, and C. L. Ives, Science **227**, 1477 (1985).
[2] J. A. Frangos, T. Y. Huang, and C. B. Clark, Biochem. Biophys. Res. Commun. **224**, 660 (1996).
[3] H. W. Sill, Y. S. Chang, J. R. Artman, J. A. Frangos, T. M. Hollis, and J. M. Tarbell, Am. J. Physiol., Heart Circ. Physiol. **268**, H535 (1995).
[4] L. Demaio, Y. S. Chang, T. W. Gardner, J. M. Tarbell, and D. A. Antonetti, Am. J. Physiol., Heart Circ. Physiol. **281**, H105 (2001).
[5] S. Sheikh, G. E. Rainger, Z. Gale, M. Rahman, and G. B. Nash, Blood **102**, 2828 (2003).
[6] T. K. Hsiai, S. K. Cho, P. K. Wong, M. Ing, A. Salazar, A. Sevanian, M. Navab, L. L. Demer, and C. M. Ho, FASEB J. **17**, 1648 (2003).
[7] S. Weinbaum, X. Zhang, Y. Han, H. Vink, and S. C. Cowin, Proc. Natl. Acad. Sci. U.S.A. **100**, 7988 (2003).
[8] N. Resnick, H. Yahav, and A. Shay-Salit, Prog. Biophys. Molec. Biol. **81**, 177 (2003).
[9] B. P. Helmke, R. D. Goldman, and P. F. Davies, Circ. Res. **86**, 745 (2000).
[10] S. A. Berger, W. Goldsmith, and E. R. Lewis, *Introduction to Bioengineering* (Oxford University Press, Oxford, 1996).
[11] A. L. Hazel and T. J. Pedley, Biophys. J. **78**, 47 (2000).
[12] A. S. Popel and P. C. Johnson, Annu. Rev. Fluid Mech. **37**, 43 (2005).
[13] B. Das, P. C. Johnson, and A. S. Popel, Biorheology **37**, 239 (2000).
[14] C. Pozrikidis, *Boundary Integral and Singularity Methods for Linearized Viscous Flow* (Cambridge University Press, Cambridge, 1992).
[15] G. P. Muldowney and J. J. L. Higdon, J. Fluid Mech. **298**, 167 (1995).
[16] P. Dimitrakopoulos and J. J. L. Higdon, J. Fluid Mech. **377**, 189 (1998).
[17] C. Pozrikidis, *Modeling and Simulation of Capsules and Biological Cells* (Chapman and Hall, London, 2003).